Modulated Control Barrier Function for Freezing Problem in Social Navigation

Yifan Xue[1], Anusha Srikanthan[1], Ze Zhang[2] and, Nadia Figueroa[1] *Member, IEEE*

***Abstract*—As prominent real-time safety-critical reactive control techniques, Control Barrier Function Quadratic Programs (CBF-QPs) work for control affine systems in general but result in freezing problems (or local minima) in social navigation and consequently cannot ensure convergence to a goal. Here, we propose on-manifold Modulated CBF-QP controllers to realize local-minimum-free reactive obstacle avoidance for control affine systems in general. We validate our methods by simulating our robot in static and dynamic human crowds using an underactuated robot modeled as a unicycle. Modulated CBF-QP outperforms CBF-QP, and MPC-CBF in all experiments, ensuring both safety and task completion.**

I. Introduction

Social robot navigation deals with the motion of robots through crowded human environments. This continues to remain a challenging problem for safe control design [1] due to the robot "freezing" along its path. The "freezing robot problem" (FRP) intuitively describes scenarios where the robot stops or starts oscillating indefinitely when the obstacle avoidance module cannot find a collision-free trajectory forward [2, 3, 1]. Over the years, many works have been proposed to reduce FRP in social navigation by either improving the human motion prediction module or the obstacle avoidance strategy. The authors of [2] approach FRP by modeling human-robot interaction during the path planning phase, where both pedestrians and the robot cooperate to adjust their path. Prior work from [4] identified that human clusters standing between the robot and the target may potentially lead to a robot freezing problem, and proposed the idea of designating a Potential Freezing Zone (PFZ), a conservative spatial zone where the robot might freeze and be obtrusive to humans. The authors then proposed a solution to avoid PFZ constructed from convex approximations of estimated cluster positions. Moreover, [5] dynamically shifts between the three policies of Go-Solo, Follow-other, and Stop using Multi-Policy Decision Making.

Existing literature has demonstrated empirically the effect of concave obstacle or concave-geometry cluster's impeding effects on target reaching for various obstacle avoidance modules. For example, [4] acknowledges that deep-reinforcement-learning-based obstacle avoidance policy leads to freezing problems when multiple humans cluster in a C-shaped formation. [6] discusses how Control Barrier Function (CBF) controllers get stuck at the saddle regions when two circular obstacle regions overlay partially into a concave geometry. However, few controllers have been designed to efficiently circumvent arbitrary concave obstacle geometries given any control affine robot system. Frozone filter in [4] does not explicitly take into consideration the robot model and actuation limits, and is not applicable when the initial location of the robot is inside its computed PFZ. While Mod-DS approach in [7] can eliminate saddle region formation facing concave obstacles but is restricted to fully actuated robot dynamics.

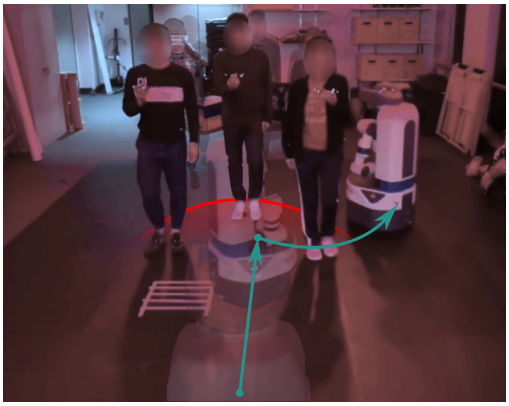

Fig. 1: Real-life experiment using MCBF-QP to reduce freezing problem in social navigation facing pedestrians moving in groups.

To address FRP and realize robust navigation facing human clusters of any geometry in social navigation for any control-affine system, we propose on-manifold Modulated CBF-QP controllers by combining CBF-QPs, the safety filter adaptable to control affine system in general, with Mod-DSs, the closed form obstacle avoidance approach capable of efficiently circumventing concave obstacles in fully-actuated system [7]. If properly tuned, the proposed Mod-based QP method is able to eliminate geometry-originated freezing problems in highly interactive environments. Additionally, on-manifold Modulated CBF-QP methods, like CBF-QP, are applicable to control-affine systems in general.

II. Preliminaries

A. Definition of Safety in Social Navigation

In this work, we define the notion of robot safety and generate safe control algorithms based on boundary functions. Given a continuously differential function h_o for an obstacle o in the detected obstacle set O, state $x \in \mathbb{R}^d$ and obstacle state $x_o \in \mathbb{R}^{d'}$, $h_o : \mathbb{R}^d \times \mathbb{R}^{d'} \to \mathbb{R}$ is a boundary function if the safe set C_o (outside the obstacle), the boundary set ∂C_o (on

[1]Y. Xue, A. Srikanthan and N. Figueroa are with the University of Pennsylvania, Philadelphia, PA 19104 USA {yifanxue, sanusha, nadiafig}@seas.upenn.edu

[2]Ze Zhang is with Chalmers University of Technology, 41296 Gothenburg, Sweden {zhze}@chalmers.se

the boundary of the obstacle), and the unsafe set $\neg C_o$ (inside the obstacles) of the system are defined as in (1), (2), (3) [8].

$$C_o = \{x \in \mathbb{R}^d, x_o \in \mathbb{R}^{d'} : h_o(x, x_o) > 0\} \tag{1}$$

$$\partial C_o = \{x \in \mathbb{R}^d, x_o \in \mathbb{R}^{d'} : h(x, x_o) = 0\} \tag{2}$$

$$\neg C_o = \{x \in \mathbb{R}^d, x_o \in \mathbb{R}^{d'} : h(x, x_o) < 0\} \tag{3}$$

In practice, $h_o(x, x_o)$ is often measured as the distance from the controlled agent to the obstacle surface boundary, i.e. the signed distance function. Given environments defined by boundary functions, the goal of a safety-critical controller is to generate an admissible input u that will ensure that the state of the robot x is always within the safe set C defined in (4) and eventually reach a target state.

$$C = \{x \in \mathbb{R}^d, x_o \in \mathbb{R}^{d'} : h_o(x, x_o) > 0, \forall o \in O\}. \tag{4}$$

B. Control Barrier Functions

In CBF-QP formulation, the boundary function $h_o(x, x_o)$ is also called the barrier function. Control Barrier Functions are designed by extending Nagumo set invariance theorem to a "control" version [8], where the condition $\forall x \in \partial C_o$ is rewritten mathematically using an extended $\mathcal{K}_\infty$ function α,

$$\begin{aligned} C_o \text{ is set invariant } \iff \exists u \text{ s.t. } & \dot{h}_o(x, x_o, \dot{x}_o, u) \\ & \geq -\alpha(h_o(x, x_o)). \end{aligned} \tag{5}$$

Control barrier functions can be generalized to any nonlinear affine systems of the form,

$$\dot{x} = f(x) + g(x)u \tag{6}$$

where $x \in \mathbb{R}^d, x_o \in \mathbb{R}^{d'}, u \in \mathbb{R}^p$, and f, g are Lipschitz continuous. The CBF condition in (5) can be used to formulate a quadratic programming problem that guarantees safety by enforcing the set invariance of the safety set C_o defined in (1). For general control affine systems, CBF-QP is defined as in (7b), where L_f and L_g are the Lie derivatives of h_o. $L_f h_o = \nabla_x h_o \cdot f(x)$ and $L_g h_o = \nabla_x h_o \cdot g(x)$.

$$u_{\text{cbf}} = \underset{u \in \mathbb{R}^p}{\arg\min}\ (u - u_{\text{nom}})^\top (u - u_{\text{nom}}) \tag{7a}$$

$$\begin{aligned} L_f h_o(x, x_o) + L_g h_o(x, x_o) u + \nabla_{x_o} h_o(x, x_o) \dot{x}_o \\ \geq -\alpha(h_o(x, x_o)) \quad \forall o \in O \end{aligned} \tag{7b}$$

C. Local Minimum and Freezing Problem

In social navigation, the term "freezing robot problem" (FRP) includes all scenarios where the robot stops or starts oscillating indefinitely facing obstacles. FRP occurs either when the obstacle avoidance module fails completely as no action can prevent the robot from entering unsafe regions in the next timestep or when, despite being feasible, the solver cannot generate a path that reasonably circumvents the surrounding obstacles due to potentially the concavity of the obstacle geometries. In the field of reactive safe controllers, researchers are interested in the latter group of FRP, which they refer as local minima or saddle points [9, 7]. In CBF-QPs, a local minimum occurs when $\dot{x}_{\text{cbf}} = f(x) + g(x)u_{\text{cbf}} = 0$ due to the safety constraints in (7b) even while the problem remains feasible.

D. Research Statement

Define $H_o(x, x_o)$ to be an orthonormal basis spanning the hyperplane tangent to the function $h_o(x|x_o)$ at point x. Here function $h_o(x, x_o)$ is written as $h_o(x|x_o)$ to indicate that the tangent is taken with respect to robot state x only. By definition, $H_o(x, x_o)$ and the gradient of the function $h_o(x, x_o)$, $\nabla_x h(x, x_o)$, constitute an orthonormal basis that fully spans the robot state space $\mathbb{R}^d$. This means that local minimum issue $\dot{x} = 0$ would only occur if and only if the projections of $\dot{x}$ onto $H_o(x, x_o)$ and onto $\nabla_x h_o(x, x_o)$ are simultaneously 0. Therefore, we can formally define the geometry-originated FRP in CBF-QPs as follows:

Given any robot's initial state inside the safe region (4), our aim is to prevent FRP by introducing tangent hyperplane guidance into regular CBF-QPs, ensuring $H_o(x, x_o) \cdot (f(x) + g(x)u) \neq 0$ when $\nabla_x h_o(x, x_o) \cdot (f(x) + g(x)u) = 0$ is enforced by the CBF-constraints in (7b), given any $o \in O$. Here $f(x) + g(x)u$ is the robot dynamics as defined in (6).

III. On-Manifold MCBF for Concave Obstacle Avoidance

Standard CBF constraints ensure robot safety by regulating $\dot{x}$ projection onto the gradient direction $\nabla_x h_o$, which is normal to the safe region h_o defined, similar to closed-form obstacle avoidance approach of on-manifold Modulation [7]. However, unlike CBF-QP that are easily trapped in saddle points, on-manifold Modulation is able to eliminate undesirable equilibrium by modulating the directions of $\dot{x}$ projected onto the hyperplane $H(x, \bar{h})$, where $\bar{h}(x)$ is the combined barrier function obtained by leveraging all boundary representations $\{\forall h_o(x, x_o), o \in U\}$ close to the robot (subsection III-A). $H(x, \bar{h})$ is an orthonormal basis tangent to $\bar{h}(x)$.

The application of on-manifold Modulation is limited to fully-actuated dynamical systems. Inspired by the on-manifold Modulation, we construct on-manifold Modulated CBF-QPs (MCBF-QPs) to achieve local-minimum-free safe control for control affine systems in general, by introducing constraints on $\dot{x}$'s projection onto the selected obstacle exit direction $\phi(x, \bar{h})$ using (8). The parameter γ is a user-defined positive real number, i.e. $\gamma \in \mathbb{R}^+$. Details of how $\phi(x, \bar{h})$ is derived can be found in subsection III-B. The MCBF-QP is given below.

$$\begin{aligned} u_{\text{mcbf}} = \underset{u \in \mathbb{R}^p}{\arg\min}\ & (u - u_{\text{nom}})^\top (u - u_{\text{nom}}) \\ L_f h(x, x_o) + L_g h(x, x_o) u + \nabla_{x_o} h(x, x_o) \dot{x}_o & \\ \geq -\alpha(h(x, x_o)) \quad \forall o \in O & \\ \phi(x, \bar{h})^\top f(x) + \phi(x, \bar{h})^\top g(x) u \geq \gamma & \end{aligned} \tag{8}$$

The performance of on-manifold MCBF-QP in concave obstacle environments is validated and compared with that of the standard CBF-QP in Figure 3, assuming single-integrator robot dynamics and $u_{\text{nom}} = x - x^*$ pointing from the robot state to the target. As we will show in our results comparing the trajectories of MCBF-QP and CBF-QP controllers, MCBF-QP eliminates

local minima including those inside the Potential Freezing Zone (regions half-surrounded by the C-shape obstacle).

A. Selective Cluster Formation

Given a set of obstacle $U = \{\forall o | h_o(x, x_o) \leq b\}$, where b is the sensing range of the robot, the combined single obstacle representation can be computed using the techniques proposed in [7] as

$$\bar{h}(x) = -\frac{1}{\rho} \log \left(\sum_{o \in U} \exp\left(-\rho h_o(x, x_o)\right) \right), \tag{9}$$

where b is a threshold distance value, and ρ is a positive user-selected constant. The smaller the value of ρ, the smoother the edges in the distance field. Note that set U is not the set of obstacles that are physically connected. Instead, the resulting function $\bar{h}$ can represent multiple discrete obstacles using a single function.

B. Generalized Obstacle Exit Strategy for Control Affine System

Given combined boundary function $\bar{h}$, the obstacle exit direction $\phi(x, \bar{h})$ can be obtained as follows. Let $e^{(0)}$ be one out of m uniformly sampled candidate directions in $\mathbb{R}^d$, satisfying the requirement in (10) and subject to $e^{(0)} \notin \mathcal{N}(H(x, \bar{h}))$. Denote x_i as the i^{th} element in robot state x, $i \in \{1, 2, .., d\}$.

$$\begin{aligned} e^{(0)} &= [e_1^{(0)}, e_2^{(0)}, .., e_d^{(0)}]^\top \\ e_i^{(0)} &= 0 \quad \text{if} \quad \frac{\partial \bar{h}}{\partial x_i} = 0 \end{aligned} \tag{10}$$

A geodesic approximation method can then propogate the candidate direction $e^{(i)}$ starting at $i = 0$ using (11), to construct a first-order approximation of the obstacle surface. This first-order approximation forms a path $X = \{x^{(0)}, x^{(1)}, ..., x^{(N)}\}$ exiting the obstacle on its isosurface, where horizon $N \in \mathbb{N}$ is a natural number [7]. Function $\phi(x, \bar{h}) \in \mathbb{R}^d$ then outputs, among m candidate directions $\{e^0\}_{k=0}^m$, the one with the smallest associated potential $P^{(N)}$ from (12), where β is the step size and $p(x)$ is a user-defined reward function, as illustruted in Figure 2. In most applications, $p(x)$ can be a weighted combination of the distance from $x^{(i)}$ to the target x^* and the value of $\bar{h}(x^{(i)})$.

$$\begin{aligned} x^{(i+1)} &= \beta H(x^{(i)}, \bar{h}) H(x^{(i)}, \bar{h})^\top e^{(i)} + x^{(i)} \\ e^{(i+1)} &= \frac{H(x^{(i)}, \bar{h}) H(x^{(i)}, \bar{h})^\top e^{(i)}}{||H(x^{(i)}, \bar{h}) H(x^{(i)}, \bar{h})^\top e^{(i)}||_2} \end{aligned} \tag{11}$$

$$P^{(i+1)} = P^{(i)} + \beta p(x^{(i+1)}) \tag{12}$$

IV. Robot Experiment

In this section, the obstacle avoidance performances using MCBF-QPs proposed in section III are validated in underactuated control affine systems using the differential-drive robot (Fetch). We compare the performance of our proposed controller with standard CBF-QP [8] and Model Predictive Control with Discrete-Time Control Barrier Function (MPC-CBF) [10] in 2 social navigation scenarios through Python simulation at 20 Hz. In the first scenario, we have humans, each modeled as a cylinder of a constant radius of 0.5 m, standing in clusters of various geometries in fixed locations. In the second scenario, we add complexity to the navigation tasks by allowing humans to be dynamic, banding, and disbanding from time to time. Robot Fetch is modeled using the standard unicycle model as in (13), derived from choosing a point of interest $a > 0$ m ahead of the wheel axis of Fetch. p_x and p_y are robot locations in x and y axis, and θ is the robot's orientation in radians measured with respect to the positive x axis. Lastly, we validated our proposed method in real-life social navigation experiment using the robot Fetch to avoid a 3-person cluster while reaching the target. We used Vicon trackers to acquire real-time human positions and velocities for the hardware experiment.

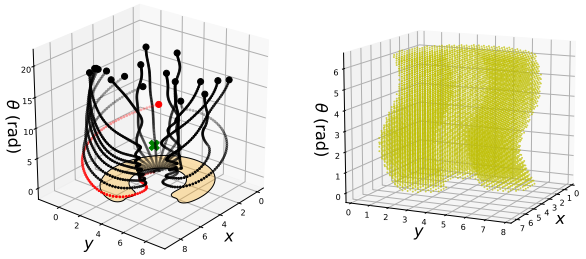

Fig. 2: Illustration of how the geodesic approximation strategy propagates 20 uniformly sampled candidate directions $e^{(0)}$ to form 20 paths Xs, and selects the optimal candidate $\phi(x, \bar{h})$ to be $e^{(0)}$ that initiates the lowest penalty path, colored in red.

$$\dot{x} = \begin{bmatrix} \dot{p}_x \\ \dot{p}_y \\ \dot{\theta} \end{bmatrix} = \begin{bmatrix} \cos\theta & -a\sin\theta \\ \sin\theta & a\cos\theta \\ 0 & 1 \end{bmatrix} \begin{bmatrix} v \\ \omega \end{bmatrix} \tag{13}$$

The control barrier function $h(x, x_o)$ for the shifted unicycle model is defined as follows, where $x_o = [p_{x_o}, p_{y_o}]^\top$ is the position of the human and c_r is the radius of the approximated cylinder.

$$h_o(x, x_o) = \sqrt{([p_x; p_y] - x_o)^\top ([p_x; p_y] - x_o)} - c_r \tag{14}$$

A. Results

In Python simulations, the trajectories produced by standard CBF-QP and the proposed MCBF-QP are illustrated in Figure 4 and Figure 5. At each point in time, MCBF-QP utilizes geodesic approximation in subsection III-B to evaluate potential exit paths $X = \{x^{(0)}, x^{(1)}, ..., x^{(N)}\}$ alongside the blue isoline depicted in the first row images of Figure 5. The best $e^{(0)}$ candidate, i.e. $\phi(x, \bar{h})$, resulting in the smallest penalty value $P^{(N)}$ is visualized as the red arrow. In the static scenario, MCBF-QP reaches the target location in an efficient trajectory while the V-shape formation of the crowds traps CBF-QP and MPC-CBF. In the more challenging dynamic social navigation test, MCBF-QP, guided by the exit direction $\phi(x, \bar{h})$, successfully circumvents the shifting and deforming cluster of humans, while CBF-QP and MPC-CBF end up colliding with the closing-up crowds. Therefore, we demonstrate that in comparison to the standard CBF-QPs, the proposed MCBF-QP

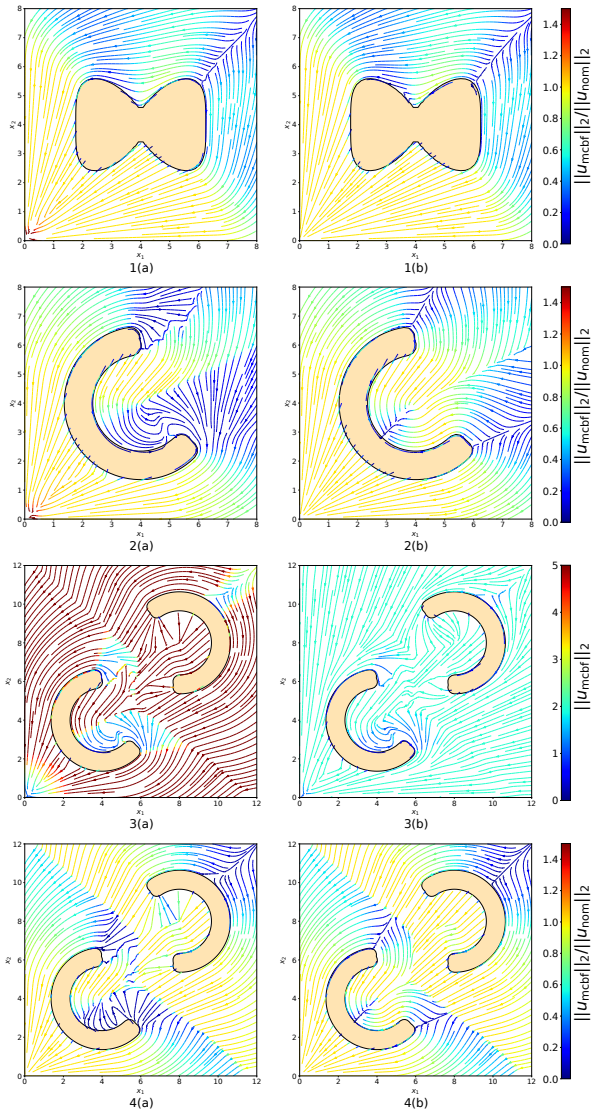

Fig. 3: Performance of on-manifold MCBF-QP (a) and CBF-QP (b) in single star-shaped (first row) and non-star-shaped (second row) obstacle avoidance with no robot input constraints. Performance of MCBF-QP in multi-concave obstacle avoidance(third row, (a): without input constraints, (b): with robot input constraints of $||u_{\text{mcbf}}||_2 \leq 2$), given $\gamma = 1$. Lastly, pictures on the fourth row show the effects of γ sizes on the resulted safe trajectories ((a): $\gamma = 0.1$, (b): $\gamma = 10$).

is more robust and successfully alleviates the freezing problem in social navigation.

In real-life hardware validation, we successfully reproduce the dynamic simulation's result using MCBF-QP to navigate around a dynamic cluster formed by 3 humans walking together. As suggested in Figure 1, MCBF-QP is capable of circumventing concave human clusters in social navigation without inducing robot freezing problems.

V. Conclusion

In this work, we proposed MCBF-QP that can successfully alleviate local minimum issues under the freezing robot problem. The current obstacle avoidance controller is limited without incorporating human motion prediction into the control pipeline. As a result, the controller cannot guarantee that the generated trajectories are the most efficient and will never lead to future freezing problems in dynamic environments. To improve our approach, we plan on incorporating the obstacle avoidance module of MCBF-QP with human motion prediction using neural networks.

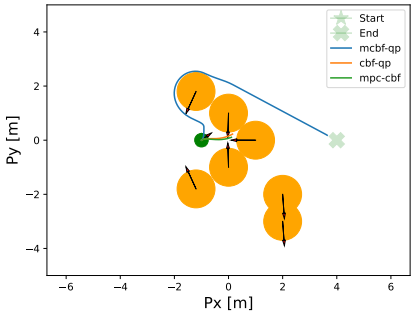

Fig. 4: Comparison of the trajectories generated by regular CBF-QP and the proposed MCBF-QP, CBF-QP and MPC-CBF. MCBF-QP managed to avoid the human crowds gathering together with an efficient path, while CBF-QP and MPC-CBF froze.

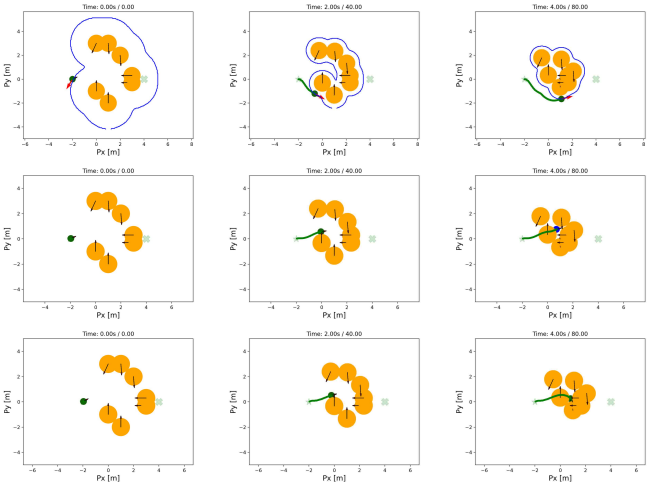

Fig. 5: Comparison of MCBF-QP (first row), CBF-QP (second row) and MPC-CBF (third row) with a horizon size of 20 performances in a challenging dynamic social navigation task. The blue contour lines in the first-row images indicate the isosurface geodesically approximated to select the proper obstacle exit strategy $\phi(x, \bar{h})$, depicted as the red arrow.

References

[1] C. Mavrogiannis, F. Baldini, A. Wang, D. Zhao, P. Trautman, A. Steinfeld, and J. Oh, "Core challenges of social robot navigation: A survey," *J. Hum.-Robot Interact.*, vol. 12, no. 3, Apr. 2023. [Online]. Available: https://doi.org/10.1145/3583741

[2] P. Trautman and A. Krause, "Unfreezing the robot: Navigation in dense, interacting crowds," in *2010 IEEE/RSJ*

International Conference on Intelligent Robots and Systems, 2010, pp. 797–803.

[3] P. Trautman, J. Ma, R. M. Murray, and A. Krause, "Robot navigation in dense human crowds: Statistical models and experimental studies of human–robot cooperation," *The International Journal of Robotics Research*, vol. 34, no. 3, pp. 335–356, 2015. [Online]. Available: https://doi.org/10.1177/0278364914557874

[4] A. J. Sathyamoorthy, U. Patel, T. Guan, and D. Manocha, "Frozone: Freezing-free, pedestrian-friendly navigation in human crowds," *IEEE Robotics and Automation Letters*, vol. 5, no. 3, pp. 4352–4359, 2020.

[5] D. Mehta, G. Ferrer, and E. Olson, "Autonomous navigation in dynamic social environments using multi-policy decision making," in *2016 IEEE/RSJ International Conference on Intelligent Robots and Systems (IROS)*, 2016, pp. 1190–1197.

[6] M. F. Reis, A. P. Aguiar, and P. Tabuada, "Control barrier function-based quadratic programs introduce undesirable asymptotically stable equilibria," *IEEE Control Systems Letters*, vol. 5, no. 2, pp. 731–736, 2021.

[7] C. K. Fourie, N. Figueroa, and J. A. Shah, "On-manifold strategies for reactive dynamical system modulation with nonconvex obstacles," *IEEE Transactions on Robotics*, vol. 40, pp. 2390–2409, 2024.

[8] A. D. Ames, S. Coogan, M. Egerstedt, G. Notomista, K. Sreenath, and P. Tabuada, "Control barrier functions: Theory and applications," in *2019 18th European control conference (ECC)*. IEEE, 2019, pp. 3420–3431.

[9] L. Huber, A. Billard, and J.-J. Slotine, "Avoidance of convex and concave obstacles with convergence ensured through contraction," *IEEE Robotics and Automation Letters*, vol. 4, no. 2, pp. 1462–1469, 2019.

[10] J. Zeng, B. Zhang, and K. Sreenath, "Safety-critical model predictive control with discrete-time control barrier function," in *2021 American Control Conference (ACC)*, 2021, pp. 3882–3889.